

# A Facile Non-hydrothermal Fabrication of Uniform $\alpha$ -MoO<sub>3</sub> Nanowires in High Yield

Banghua Qi,<sup>1,2</sup> Xiaomin Ni,<sup>\*3</sup> Dongguo Li,<sup>1</sup> and Huagui Zheng<sup>\*1</sup>

<sup>1</sup>Department of Chemistry, University of Science and Technology of China, Hefei, Anhui 230026, P. R. China

<sup>2</sup>Anhui Science and Technology University, Fengyang, Anhui 233100, P. R. China

<sup>3</sup>State Key Lab of Fire Science, University of Science and Technology of China, Hefei, Anhui 230026, P. R. China

(Received January 7, 2008; CL-080006; E-mail: nxmin@ustc.edu.cn, hgzheng@ustc.edu.cn)

Uniform  $\alpha$ -MoO<sub>3</sub> nanowires with the diameter of 60–100 nm and the length of 10–40  $\mu$ m were fabricated in high yield through a facile non-hydrothermal method. The fabrication process involved acidifying an ethylenediamine solution of molybdenum acid and subsequent calcinating treatment without any hydrothermal procedures. Ethylenediamine was found to play a crucial role for the formation of  $\alpha$ -MoO<sub>3</sub> nanowires under the present conditions. Thus-prepared  $\alpha$ -MoO<sub>3</sub> nanowires as supercapacitors exhibited much larger capacitance and better cyclicity than the conventional particulate counterpart.

Nanosized molybdenum oxides have been of great interest for their wide applications in catalytic, optical, and electrochemical fields.<sup>1–3</sup> Generally, MoO<sub>3</sub> has three phases of  $\alpha$ ,  $\beta$ , and  $h$ . In all these MoO<sub>3</sub> structures, MoO<sub>6</sub> octahedron is the basic building unit. For orthorhombic  $\alpha$ -MoO<sub>3</sub>, the MoO<sub>6</sub> octahedra share edges and corners, resulting in a zigzag chain and a unique layer structure.<sup>4</sup> Monoclinic  $\beta$ -MoO<sub>3</sub> has a ReO<sub>3</sub>-related structure, in which the MoO<sub>6</sub> octahedra share corners to form a distorted cube.<sup>5</sup> Hexagonal  $h$ -MoO<sub>3</sub> is constructed from the same zigzag chains of MoO<sub>6</sub> octahedra which connected through the cis-position.<sup>6</sup> Among them,  $\alpha$ -MoO<sub>3</sub>, as the thermodynamically stable phase, was paid most attention. To date, various methods have been exploited for the fabrication of  $\alpha$ -MoO<sub>3</sub> nanostructures, such as nanowires produced by electrospinning technique,<sup>7</sup> nanorods fabricated by heating a Mo foil with infrared irradiation,<sup>8</sup> nanobelts created by oxidizing Mo powders with H<sub>2</sub>O<sub>2</sub>,<sup>9</sup> nanoslabs made via microwave plasma-enhanced chemical vapor,<sup>10</sup> and nanofibers prepared through the hydrothermal treatments.<sup>11</sup> In these methods, the solution route is probably the most used for its simplicity and high yield. However, hydrothermal treatments and long aging time are usually involved in solution routes.<sup>12</sup> In this work, we report a non-hydrothermal method for the fabrication of uniform  $\alpha$ -MoO<sub>3</sub> nanowires in ethylenediamine as an organic base, which proved to be convenient, timesaving, and low cost.

All reagents were analytical grade. In a typical experiment, 12 mmol of H<sub>2</sub>MoO<sub>4</sub>·H<sub>2</sub>O was dissolved in 20 mL of aqueous solution containing 4 mol·L<sup>–1</sup> ethylenediamine. Then, diluted acid solution was added dropwise to obtain a large amount of white precipitate. Subsequently, the resulting white powder was filtered off, dried and finally calcined at 360 °C for 4 h.

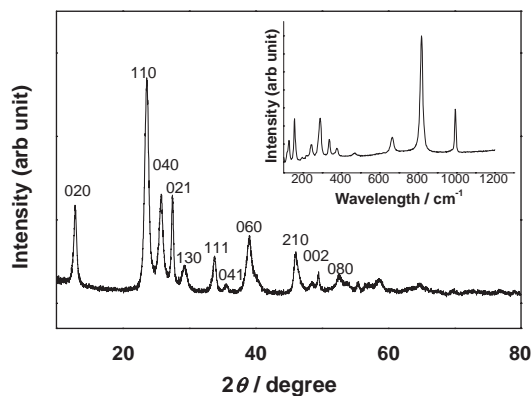
X-ray diffraction was carried out on a Philips X'Pert Super diffractometer with graphite monochromatized Cu K $\alpha$  radiation ( $\lambda$  = 1.54178 Å). The Raman spectrum was collected at ambient temperature on a SPEX 1403 spectrometer with an argon-ion laser at an excitation wavelength of 514.5 nm. The morphology of the product was examined by a field emission scanning electron microscope (FE-SEM, JEOL JSM-6300F) and a high-

resolution transmission electron microscope (HRTEM, JEOL-2010) with accelerating voltage of 200 kV. The electrochemical capacitance of the sample was tested using a cell of symmetrical configuration in a galvanostatic charge–discharge model with a constant current of 5 mA.

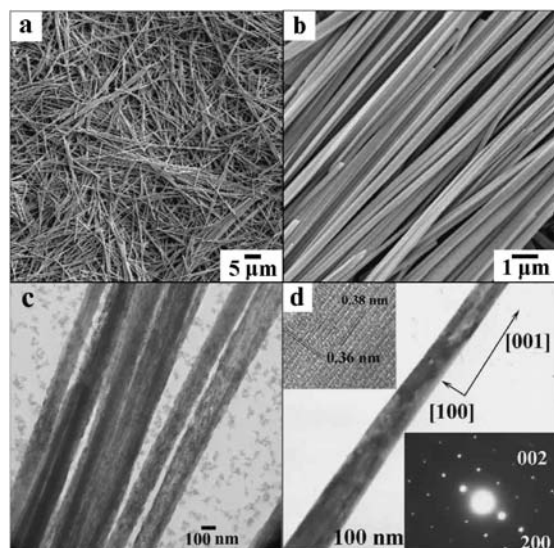
Figure 1 shows the XRD pattern of the resulting product, which could be well indexed as orthorhombic phase MoO<sub>3</sub> (JCPDS: 05-0508). The difference between observed intensities of the diffraction peaks and those reported in the JCPDS card implied the orientated growth of as-prepared sample considering the fact that the product was characterized with XRD without grinding. Inset is the corresponding Raman spectrum, in which the three peaks at 997, 821, and 667 cm<sup>–1</sup> are assigned to the stretching mode of the terminal Mo=O groups and the asymmetric and symmetric stretching modes of the Mo–O–Mo bridges in  $\alpha$ -MoO<sub>3</sub>, respectively.<sup>13</sup> Both the results indicate that  $\alpha$ -MoO<sub>3</sub> was produced by the present procedures.

Figure 2 shows the morphology of the sample. SEM images of Figures 2a and 2b reveal that the sample consisted of nanowires with a length of 10–40  $\mu$ m and a diameter of 60–100 nm. The TEM image in Figure 2c shows nanowires, agreeing well with the morphological characteristics observed by FE-SEM. The corresponding selected-area electron diffraction (SAED) pattern taken from a single wire reveals the single crystalline nature of the wire with growth orientation of [001]. The crystal lattice fringes of 0.38 and 0.36 nm shown in the HRTEM image of Figure 2d corresponded to the (001) and (100) planes, further proving the above SAED result.

It was found that the solvent ethylenediamine played an important role for the formation of the  $\alpha$ -MoO<sub>3</sub> nanowires without any hydrothermal process. In the current system, ethylenediamine acts as an organic alkali solvent to dissolve the precursor hydrated molybdic acid, which differs from the



**Figure 1.** XRD pattern of the  $\alpha$ -MoO<sub>3</sub> sample, inset was the corresponding Raman spectrum.



**Figure 2.** Morphological images of the  $\alpha$ - $\text{MoO}_3$  sample. (a) A panoramic SEM image of the sample. (b) Magnified SEM image of the sample. (c) TEM image of the nanowires. (d) A typical TEM image of the nanowire, inset were the corresponding HRTEM image and SAED pattern.

conventional inorganic solvent of ammonia solution. In the following acidifying procedure, molybdic acid intermediate would precipitate as the acidity of the system increases. During this process, a large quantity of heat was released from the reaction between ethylenediamine and hydrogen ions, which raised the system temperature to  $105^\circ\text{C}$ . Thus, precipitated molybdic acid crystallized and the crystals grew at a relatively fast rate, avoiding further hydrothermal treatments or long aging time. On the other hand, ethylenediamine as a strong coordinating solvent is believed to play the role of structure-directing agent.<sup>14</sup> Control experiments showed that only irregular particles could be obtained without the assistance of ethylenediamine. As a result, ethylenediamine was considered to act as both the solvent and structure-directing agent in the formation of  $\alpha$ - $\text{MoO}_3$  nanowires. But the reason is not clear and further research is in progress.

The electrochemical properties of the nanowires and a commercial sample as electrochemical double-layered supercapacitors (EDLSCs) were studied by galvanostatic tests at room temperature. Figure 3 gives the typical charge/discharge curves (inset) and the cyclic performance of the two samples. Our nanowires obviously displayed much higher specific capacitance and better cyclic stability than that of the particulate sample. For the nanowires, the initial charge/discharge capacitance reached  $386\text{ F}\cdot\text{g}^{-1}$  and about 82% of initial discharge capacitance was reserved after 150 charge/discharge cycles. However, for the conventional particles, the first charge/discharge capacitance was only 58% of the nanowires and the capacitance decreased rapidly. Furthermore, our sample also exhibited better performance than that of the nanobelts prepared by other methods.<sup>15</sup> Two possible explanations can be provided for the improved electrochemical performances of as-obtained  $\alpha$ - $\text{MoO}_3$  nanowires. One is that the movement of electrons in the electrode materials is diffusion limited, which is a kinetic factor. The diffusion length of electrons in the  $\text{MoO}_3$  nanowires is much

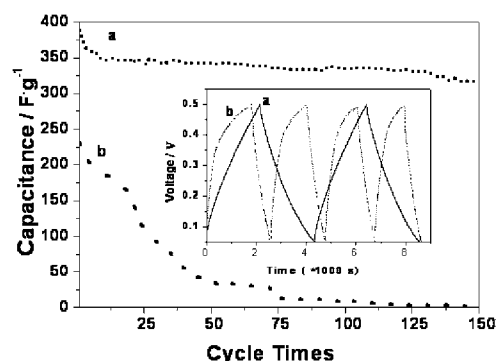


**Figure 3.** The cycle performance and typical charge-discharge curves (inset) of (a) as-prepared  $\alpha$ - $\text{MoO}_3$  nanowires, (b) commercial  $\alpha$ - $\text{MoO}_3$  particles.

shorter than that of bulk materials, which is beneficial for the electrode kinetics and favors the charge-transport process in the charge/discharge cycles.<sup>16</sup> Another explanation is the higher surface area of the  $\text{MoO}_3$  nanowires ( $78.2\text{ m}^2\cdot\text{g}^{-1}$ ) compared to that of the particulate sample ( $16.7\text{ m}^2\cdot\text{g}^{-1}$ ), which allows larger active surface reached by the electrolyte ions.<sup>17</sup> The one-dimensional nanostructured electrode materials are considered the smallest dimensional structures for efficient electron transport, thus leading to their superior electrochemical performance compared with other morphological electrode materials.<sup>18</sup>

In summary, uniform  $\alpha$ - $\text{MoO}_3$  nanowires have been created in high yield through a simple non-hydrothermal method in ethylenediamine. The structure, morphology, and electrochemical properties of the nanowires were investigated. Such  $\alpha$ - $\text{MoO}_3$  nanowires are expected to find applications in the fields of electrochemical materials, catalyst, and optics considering their nanosize and unique shapes.

## References and Notes

- 1 S. T. Oyama, W. Zhang, *J. Am. Chem. Soc.* **1996**, *118*, 7173.
- 2 S. Li, M. S. El-Shall, *Nanostruct. Mater.* **1999**, *12*, 215.
- 3 W. Li, F. Cheng, Z. Tao, J. Chen, *J. Phys. Chem.* **2006**, *110*, 119.
- 4 J. Song, X. Ni, D. Zhang, H. Zheng, *Solid State Sci.* **2006**, *8*, 1164.
- 5 I. Juárez Ramirez, A. Martínez-de la Cruz, *Mater. Lett.* **2003**, *57*, 1034.
- 6 J. Guo, P. Zavtli, M. S. Whittingham, *J. Solid State Chem.* **1995**, *117*, 323.
- 7 P. Gouma, K. Kalyanasundaram, A. Bishop, *J. Mater. Res.* **2006**, *21*, 2904.
- 8 E. Comini, L. Yubao, Y. Brando, G. Sberveglieri, *Chem. Phys. Lett.* **2005**, *407*, 368.
- 9 X. Hu, D. Ma, L. Xu, Y. Zhu, Y. Qian, *Chem. Lett.* **2006**, *35*, 962.
- 10 K.-P. Chang, U.-S. Chen, H. C. Shih, *Electrochem. Solid-State Lett.* **2007**, *10*, H111.
- 11 S. Wang, Y. Zhang, X. Ma, W. Wang, X. Li, Z. Zhang, Y. Qian, *Solid State Commun.* **2005**, *136*, 283.
- 12 L. Fang, Y. Shu, A. Wang, T. Zhang, *J. Phys. Chem. C* **2007**, *111*, 2401.
- 13 G. Mestl, T. K. K. Srinivasan, *Cat. Rev.-Sci. Eng.* **1998**, *40*, 451.
- 14 Y. Li, H. Liao, Y. Ding, Y. Fan, Y. Zhang, Y. Qian, *Inorg. Chem.* **1999**, *38*, 1382.
- 15 Supporting Information is electronically available on the CSJ Journal Web Site, <http://www.csj.jp/journals/chem-lett/>.
- 16 S. Nordlinder, J. Lindgren, T. Gustafsson, K. Edström, *J. Electrochem. Soc.* **2003**, *150*, E280.
- 17 D. R. Rolison, B. Dunn, *J. Mater. Chem.* **2001**, *11*, 963.
- 18 B. Ammundsen, J. Paulsen, *Adv. Mater.* **2001**, *13*, 943.